Inversion of Seismic and Gravity Data for the Composition and Core Sizes of the Moon

V. A. Kronrod and O. L. Kuskov

Vernadsky Institute of Geochemistry and Analytical Chemistry, Russian Academy of Sciences,
ul. Kosygina 19, Moscow, 119991 Russia

Abstract—We model the internal structure of the Moon, initially homogeneous and later differentiated due to partial melting. The chemical composition and the internal structure of the Moon are retrieved by the Monte-Carlo inversion of the gravity (the mass and the moment of inertia), seismic (compressional and shear velocities), and petrological (balance equations) data. For the computation of phase equilibrium relations and physical properties, we have used a method of minimization of the Gibbs free energy combined with a Mie-Gr@uneisen equation of state within the $CaO-FeO-MgO-Al_2O_3–SiO_2$ system. The lunar models with a different degree of constraints on the solution are considered. For all models, the geophysically and geochemically permissible ranges of seismic velocities and concentrations in three mantle zones and the sizes of Fe-10%S core are estimated. The lunar mantle is chemically stratified; different mantle zones, where orthopyroxene is the dominant phase, have different concentrations of FeO, Al_2O_3, and CaO. The silicate portion of the Moon (crust + mantle) may contain 3.5–5.5% Al_2O_3 and 10.5–12.5% FeO. The chemical boundary between the middle and the lower mantle lies at a depth of 620–750 km. The lunar models with and without a chemical boundary at a depth of 250–300 km are both possible. The main parameters of the crust, the mantle, and the core of the Moon are estimated. At the depths of the lower mantle, the *P* and *S* velocities range from 7.88 to 8.10 km/s and from 4.40 to 4.55 km/s, respectively. The radius of a Fe-10%S core is 340 ± 30 km.

*Keyword*s: the Moon, composition, temperature, internal structure, seismic velocities.

DOI: 10.1134/S1069351311070044

1. INTRODUCTION

The models of chemical and mineral composition of the lunar mantle are contradictory, depending on the particular method (geochemical or geophysical) applied. The estimates of the composition are based on the element correlations in chondrites and on the seismic and gravity constraints. Not only do the models pertaining to different model classes (geochemical and geophysical) exhibit discrepancies but also particular models within each class are inconsistent. The major disagreement relates to the concentrations of FeO and refractory oxides (Al_2O_3, CaO); FeO content is estimated to range from 6 to 18 wt % [Galimov, 2004; Lognonné, 2005; Wieszorek et al., 2006; Kuskov et al., 2009].

Of particular interest for reconstructing the composition, the internal structure, and the thermal state of the Moon is the approach that is based on seismic and gravity inversion [Kronrod and Kuskov, 1997; Kuskov and Kronrod, 1998a; 2000; 2001; Kuskov et al., 2002; Khan et al., 2000; 2006a; 2006b; 2007]. In this approach, the solution of the inverse problem involves an inversion of the known geophysical parameters for temperature and composition. The problem of joint seismic and gravity inversion is essentially nonlinear.

The optimization method for solving the inverse problem implies the minimization of the functional, which contains the misfits between the calculated and observable seismic velocities, the moment of inertia, and the mass of the Moon [Kronrod and Kuskov, 1997; Kuskov and Kronrod, 1998a; 1999].

Another approach to the problem of constitution and internal structure of the Moon was proposed by Kuskov and Kronrod [1998b]. The underlying idea behind this approach, which also includes solving the inverse problem and invokes seismic data, is that the outer shell of the initially homogeneous Moon had experienced partial differentiation (probably due to the formation of the magma ocean.) In other words, the magma ocean (MO) hypothesis can be used as an additional petrological constraint on the composition of the mantle in the form of balance equations for the concentrations of the main oxides. Kuskov and Kronrod [1998b] have shown that the hypothesis of differentiation of an approximately 500-km thick magma ocean into the crust of the upper and the middle mantle against the undifferentiated lower mantle agrees with the moment of inertia and the mass of the Moon. It is also consistent with the *P*- and *S*-velocity profiles presented by Nakamura [1983], where the whole body

of the seismic data provided by the Apollo-12, 14, 15, and 16 missions were analyzed and the most complete, at that moment, seismic model of the Moon was suggested.

In the present work, we suggest a new model of the constitution and internal structure of the Moon. This model is based on the hypothesis of the magma ocean; it involves modern mathematical processing of the P- and S-travel-time data [Lognonné et al., 2003; Lognonné, 2005; Gagnepain-Beyneix et al., 2006] and determining the lunar moment of inertia [Konopliv et al., 1998]. The input data for the model are the mass, the radius, the average density, the moment of inertia of the Moon, and the seismic velocities in the lunar mantle. The chemical composition of the lower (undifferentiated) mantle, which is not affected by melting, is assumed to be similar to the average composition of the overlying lunar shells and to reflect the bulk composition of the silicate portion of the Moon. This means that the outer shell of the Moon was the only source for the formation of the crust, the upper, and the middle mantle due to the differentiation of MO. That is, to construct the model, besides using the geophysical data, we also impose petrological constraints on the composition of the mantle by introducing the balance equations, which govern the distributions of the major chemical elements in the different zones of the mantle within the mineral system $CaO-FeO-MgO-Al_2O_3-SiO_2$ (CFMAS) with solid solutions. The chemical composition of the mantle and the size of the Fe-S core are inferred by the Monte-Carlo inversion procedure. The inverse problem is solved by the method of minimization of Gibbs free energy combined with the Mie-Grüneisen equation of state in the CFMAS mineral system.

2. PETROLOGICAL AND GEOPHYSICAL CONSTRAINTS

2.1. Models of the Magma Ocean

The early differentiation of the Moon with the formation of the continental feldspar crust, which has a thickness of about $50-60$ km and $\sim25\%$ Al_2O_3, as well as the age of the lunar rocks, have motivated the hypothesis of the Magma Ocean. The latter is commonly understood as the outer lunar shell, which had undergone partial melting [Ringwood, 1979; Taylor, 1986; Shearer and Papike, 1993]. The thickness of the supposed lunar Magma Ocean is estimated with a broad scatter and range from the upper $200-500$ km to the whole Moon to be molten, either partially or totally [Binder, 1986; Solomon, 1986; Wieczorek et al., 2006]. This issue is one of the key challenges in the magma evolution of the Moon, as the answer would define the composition of the zonal upper mantle and the existence of the lower primordial mantle, which is unaffected by melting.

By analyzing the thermoelastic stresses, Solomon [1986] showed that there is no tectonic evidence for a large-scale expansion or compression of the Moon over the past four billion years (after a period of its intense bombardment). He estimated the lunar radius to have been changed by about a kilometer, which disagrees with the concept of extensive melting. The set of petrological, geochemical, and geophysical data offers no reasons to believe that the Moon had ever been totally molten and formed a continuous magma ocean. This is also supported by the lunar asymmetry (the center of figure of the Moon is offset by 2 km from the center of mass). By analyzing the volumetric effects of differentiation of the Moon, Kirk and Stevenson [1989] estimate the depth of the magma ocean as 630 km. Hess and Parmentier [1995] infer a greater melting depth (800 km) from the study of the thermochemical evolution of the Moon. It has been assumed by James [1980] that during the cooling of a molten layer with a thickness of 300 km, the crystallization differentiation resulted in the formation of mafic and ultramafic cumulates in the lunar interior (the source region for mare basalts) and anorthositic crust (ferroanorthosites). The complementarity of the spectra of rear earth elements (REE) in the mare and continental rocks is believed to provide reliable support in favor of the magma ocean model [Demidova et al., 2007]. From the geochemical standpoint, a thickness of less than $300-400$ km for the magma ocean is unfeasible as, with a bulk $4-6$ wt % Al_2O_3, a smaller depth of melting would be incapable to ensure $\sim25\%$ Al_2O_3 in the anorthositic crust.

The melting depth of $500-600$ km well agrees with the experimental data on the crystallization of lunar basalts and green and picrite glass [Ringwood and Essene, 1970; Delano, 1986; Longhi, 1992; Elkins et al., 2000]. The experiments show that the mare basalts, both rich and poor in titanium, had likely been formed at similar depths (although from different sources) under the conditions of low or intermediate partial melting (<20%) and, correspondingly, the lunar mantle had not experienced extensive melting [Shearer and Papike, 1993; Head and Wilson, 1992; Wieczorek et al., 2006]. According to [Longhi 1992; Elkins-Tanton et al. 2003; Wieczorek and Phillips, 2000], the seismic boundary at a depth of 500 km can only be a local feature related to the source of mare basalts within a specific region, the Procellarum KREEP Terrane.

Some information on the thickness of MO can be inferred from the geophysical data. The results of the Apollo mission infer that one or a few seismic boundaries exist in the mantle at a depth of $400-750$ km [Goins et al., 1981; Nakamura, 1983; Lognonné et al., 2003; Lognonné, 2005; Khan et al., 2000; 2006a; 2006b; 2007; Gagnepain-Beyneix et al., 2006] (Fig. 1, Table 1.) According to the seismic stratification, the lunar mantle can be considered to be composed of two or three reservoirs separated by the boundaries, which are understood to be chemical interfaces separating
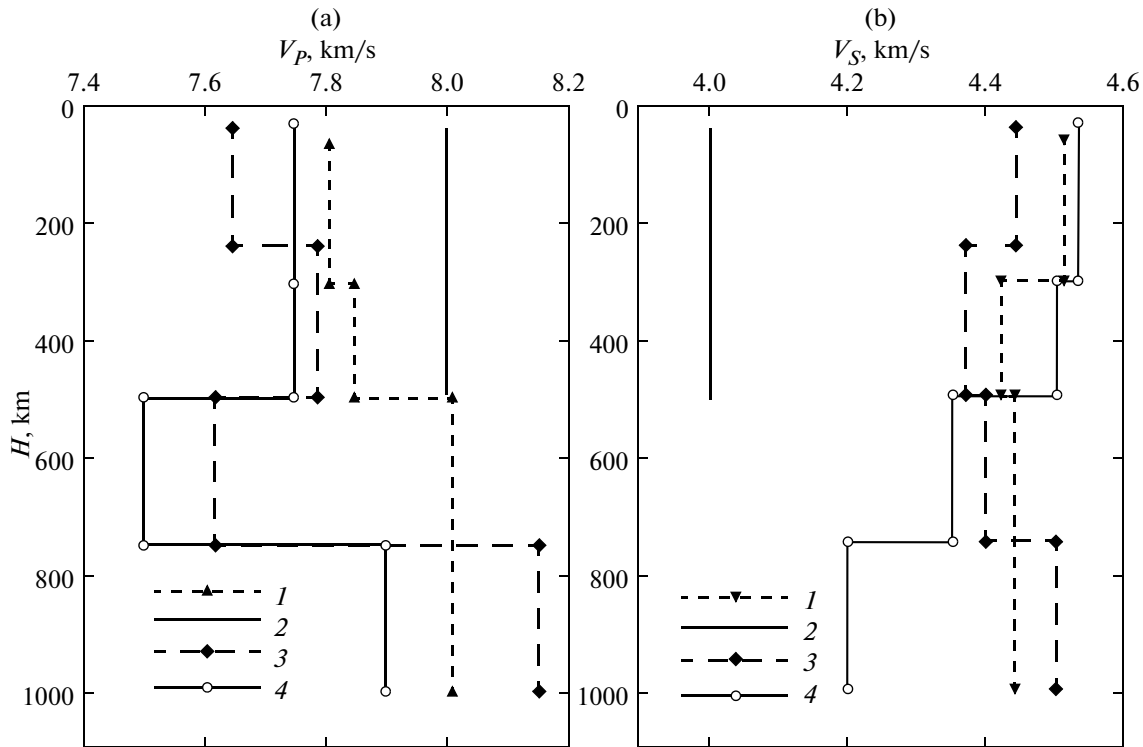
Fig. 1. Seismic velocity profiles for the longitudinal (a) and transversal (b) waves propagating in the lunar mantle. *1* according to Kuskov et al., [2002]; *2*, to Khan et al. [2000], *3*, to Gagnepain-Beyneix et al. [2006], *4*, to Lognonné et al. [2005].

the undifferentiated lower mantle from the differentiated outer shells (e.g., the upper and the middle mantle) [Kronrod and Kuskov, 1997; Kuskov and Kronrod, 1998a; 1998b].

The probable petrologic models of a seismic boundary at a depth of 500−600 km are analyzed in many works [Hood and Jones, 1987; Kuskov and Kronrod, 1998a; 1998b; Wieczorek et al., 2006]. According to one of these models, melting and subsequent differentiation occurred up to this depth. In the other model, the lunar mantle is assumed to initially have a jump in concentration at this depth, which persisted after the formation of the lunar ocean. The third model addresses the crystallization of a deep, almost global lunar ocean. In the fourth model, the seismic boundary at a depth of 500 km is understood to be the maximum depth of melting only in the lunar mare regions [Longhi 1992; Elkins-Tanton et al. 2003]. According to the estimates obtained in this model, at a depth below 500 km, the mantle should have been enriched with Al_2O_3 by 1 wt %. If this hypothesis is valid, the seismic boundary at a depth of 500 km has a regional extent.

In our works [Kronrod and Kuskov, 1997; Kuskov and Kronrod, 1998a; 1998b; Kuskov et al., 2002] based on the inversion of geophysical data, the sharp seismic boundary was referred to the alteration of the chemical composition at the depths which separate the primordial Al- and Ca-rich lower mantle from the

outer shells of the differentiated mantle. This means that the melting involved material up to a maximum depth of 500−600 km, which separates the early olivine-rich and the later orthopyroxene-rich cumulates [Wieczorek et al., 2006]. The interpretation of seismic data [Lognonné et al., 2003; Lognonné, 2005; Gagnepain-Beyneix et al., 2006; Khan et al., 2007] with the boundaries at 500−750 km leads to the same conclusion. Note that differentiation up to 500−750 km implies that all aluminum contained in the crust has been extracted from the upper lunar shells only.

2.2. Seismic Data

The seismic data are a kind of the Rosetta Stone for understanding the internal structure of the Moon. Processing the data obtained in the experiment that lasted for eight years (1969−1977) and included seismic measurements at four landing sites of Apollo-12, 14, 15, and 16 missions revealed the seismic structure of the lunar interiors shown in Fig. 1 and Table 1.

The mathematical processing of travel times of *P*- and *S* waves suggests a zonal structure of the lunar mantle. Goins et al. [1981] report on one sharp seismic contrast at a depth of about 400 km. Nakamura [1983] identifies two seismic boundaries at depths of 270 and 500 km with a distinct zone of reduced velocities in the interval of 270−500 km and a particularly highly contrasting boundary at a depth of 500 km, where the

Table 1. Seismic velocities in the lunar mantle

Model	Depth, km	V_P, km/s	V_S, km/s
[Goins et al., 1981]	60	7.75 ± 0.15	4.57 ± 0.10
	400	7.65 ± 0.15	4.37 ± 0.10
	480−1100	7.60 ± 0.15	4.20 ± 0.10
[Nakamura, 1983]	60−300	7.74 ± 0.12	4.49 ± 0.03
	300−500	7.46 ± 0.25	4.25 ± 0.10
	500−1000	8.26 ± 0.40	4.65 ± 0.16
[Khan et al., 2000]	45−500	8.0 ± 0.8	4.0 ± 0.4
	500−750	9.0 ± 1.9	5.5 ± 0.9
	750−1000	11.0 ± 2.1	6.0 ± 0.7
[Khan et al., 2007][1]	45−1000	7.75−8	4.2−4.5
[Lognonné et al., 2003]	30−300	7.75 ± 0.15	4.53 ± 0.15
[Lognonné, 2005]	300−500	7.75 ± 0.15	4.50 ± 0.15
	500−750	7.50 ± 0.30	4.35 ± 0.30
	750−1000	7.90 ± 0.30	4.20 ± 0.30
[Gagnepain-Beyneix et al., 2006]	40−240	7.65 ± 0.06	4.44 ± 0.04
	240−500	7.79 ± 0.12	4.37 ± 0.07
	500−750	7.62 ± 0.22	4.40 ± 0.11
	750−1000	8.15 ± 0.23	4.50 ± 0.10
[Kuskov, Kronrod,1998]	60−300	7.67−7.80	4.45−4.51
	400	7.53−7.60	4.29−4.30
	800	8.17−8.20	4.50−4.51
[Kuskov et al., 2002]	60−300	7.81 ± 0.40	4.51 ± 0.18
	300−500	7.85 ± 0.40	4.42 ± 0.19
	500−1000	8.01 ± 0.38	4.44 ± 0.20
Present work[2], MI model.	50−250	7.766 ± 0.06	4.51 ± 0.03
	250−625	8.03 ± 0.1	4.49 ± 0.05
	625−1000	8.073 ± 0.07	4.49 ± 0.03
Present work[3], MIS model.	50−250	7.67 ± 0.029	4.46 ± 0.01
		7.8 ± 0.06	4.51 ± 0.03
	250−625	7.84 ± 0.044	4.41 ± 0.018
		7.81 ± 0.06	4.45 ± 0.02
	625−1000	7.91 ± 0.025	4.42 ± 0.014
		7.97 ± 0.045	4.51 ± 0.03
Present work[4], MISC model	50−250	7.68 ± 0.015	4.42 ± 0.012
	250−625	7.76 ± 0.03	4.42 ± 0.01
	625−1000	7.86 ± 0.03	4.46 ± 0.01

Notes: [1] The seismic velocities are estimated from the graphs in [Khan et al., 2007], where numerical values are not cited in the text.

[2] MI model, constraints on the mass and the moment of inerti.

[3] MIS model, constraints on the mass, the moment of inertia, and the seismic velocities in the upper and the middle mantle. The estimates presented in the upper lines are the constraints according to the model of Gagnepain-Beyneix et al. [2006], and those in the lower lines, according to the model in [Lognonné et al., 2005].

[4] MISC model, constraints on the mass, the moment of inertia, and the seismic velocities in the upper and the middle mantle according to the model of Gagnepain-Beyneix et al. [2006] plus the condition of similar concentrations in the upper and the middle mantle.

[1−4] The values of the seismic velocities and the corresponding errors in the present models are the mean values and the standard deviations calculated assuming normal distributions in the frequency histograms.

P- and *S* velocities sharply increase by about 10% (in the Earth, the corresponding jumps on the seismic boundaries at 400 and 650 km are 2.5−5% for *P* velocities and 3.5−7.5% for *S* velocities).

In the recent works of Danish [Khan et al., 2000; 2006a; 2006b; 2007] and French [Lognonné, 2005; Lognonné et al., 2003; Gagnepain-Beyneix et al., 2006] geophysicists, the Appollo seismic records of *P*- and *S*-travel times have been reanalyzed [Lognonné et al., 2003] (Fig. 1). The velocity profiles [Lognonné et al., 2003; Gagnepain-Beyneix et al., 2006] show a reasonable agreement with the previous results of [Goins et al., 1981; Nakamura, 1983] at all depths, while the profiles obtained by Khan et al. [2000], only up to a depth of 500 km. In the upper mantle (up to approximately 300 km), all seismic models give practically similar seismic velocities. In the deeper horizons of the mantle, considerable discrepancies appear. For example, seismic velocities in the lower mantle (below 500−750 km) are estimated in all models with large errors attaining 0.23−0.6 km/s and 0.1−0.3 km/s for the *P* and *S* waves, respectively. Therefore, in the present work, we used only the seismic data up to a depth of approximately 500 km as the reference information.

2.3. The Crust

In a recent review, Wieczorek et al. [2006] presented a compilation of estimates for the crustal thickness of the Moon inferred from seismic, gravity, and topographic surveys. According to these estimates, the thickness of the crust is most likely 49 ± 16 km. The content of Al_2O_3 is 28.5−32% for the upper crust, 25−29% for the lower crust, and 18−25% for the bottom portions of the mafic crust, which is close to the previous estimate of 25% Al_2O_3 in the entire crust [Taylor, 1982]. According to seismic data, the anorthositic crust is 30−60 km thick [Nakamura, 1983; Lognonné et al., 2003; Khan et al. 2006a; 2006b; 2007; Gagnepain-Beyneix et al., 2006]. In the present work, instead of the anorthositic lunar crust with a nonuniform thickness, we use a 50-km thick spherical shell, which is uniform in chemical composition, density and thickness [Khan et al., 2006a; 2006b; Wieczorek et al., 2006] (Table 2). The crustal composition (wt %), according to [Taylor, 1982], includes 25% Al_2O_3, 16.5% CaO, 7% MgO, 6.5% FeO, and 45.5% SiO2. The crustal density was specified to be 2.9 g/cm^3 according to the crustal models from [Wieczorek et al., 2006] and the series of preliminary calculations where the compliance with the model constraints was the criterion of the best fit.

2.4. The Mantle

In the present work, in the modeling of the chemical composition of the Moon, we considered three intervals of oxide concentrations in the upper, middle, and lower mantle (wt %):

$$28 \le MgO \le 43\%, \ 40 \le SiO_2 \le 58\%, \ 7 \le FeO \le 16\%,$$

$$1 \le Al_2O_3 \le 8\%, \ CaO = 0.8c(Al_2O_3).$$

Determinations of the seismic parameters and electric conductivity show that up to a depth of 1200−1400 km, the lunar mantle is solid and does not contain disseminated melt inclusions [Latham et al., 1975; Nakamura, 1983]. The existence of mascons also imposes similar requirements: the thickness, the viscosity, and the mechanical properties of the underlying layers should be sufficient for the material to withstand the load in the form of mascones. The upper mantle has a high viscosity ($\sim 10^{26-27}$ P), which corresponds to a high seismic *Q* factor ($Q = 4000−7000$ for *P*-, *S* waves up to a depth of 500 km) [Arkani-Hamed, 1973; Nakamura and Koyama, 1982]. As the depth increases, the viscosity significantly decreases.

2.5. The Core

Following [Kuskov and Kronrod, 2000; 2001; Kuskov et al., 2009], we will consider the model of the internal structure of the Moon with an iron sulfide core containing 10 wt% sulfur (Fe-10 wt %S core, $Fe_{0.84}S_{0.16}$), density $\rho = 5.7$ g/cm^3 under a pressure of 50 kbar, and temperature of 1500°C.

2.6. Temperature and Pressure

The high *Q* factor of the lunar interiors [Arkani-Hamed, 1973; Nakamura and Koyama, 1982], the data on electric conductivity of the Moon [Vanyan and Egorov, 1977], and the existence of mascones and deep-focus moonquakes [Latham et al. 1972; Lognonné, 2005] suggest that the temperature distribution in the lunar mantle is likely below the solidus temperature. In our works [Kronrod and Kuskov, 1997; 1999; Kuskov et al., 2002] (Fig. 2), the thermal conditions were reconstructed using the following temperature distribution in the lunar mantle:

$$T°C = T_{60} + A \times \{1 − EXP[B \times (60 − H)]\}, \quad (1)$$

where *H* is depth in km and T_{60} is temperature at a depth of 60 km. The temperature intervals at a depth of 60, 270, 500, and 800 km are, respectively, 430−470°C, 770−850°C, 1000−1100°C, and 1200−1250°C. In [Kuskov and Kronrod, 2009], the following temperature profile was inferred from the geochemical and seismic data:

$$T°C = 351 + 1718 \times (1 − \exp(−0.00082 \times H). \quad (2)$$

The published data on the temperature distributions in the lunar mantle suggest the following values: 750°C at a depth of 500 km, 1200°C at 800 km, and 1400°C at 1100 km [Hood and Zuber, 2000]; 810−825°C at a depth of 400 km and 1175−1250°C at 1000 km [Gagnepain-Beyneix et al., 2006], Fig. 2. In

Table 2. Parameters of the models

		Main input paramerters		
Parameter	Description	Value	Note	
R_{Moon}	Radius of the Moon	1738 km	[Konopliv et al., 1998]	
I_{Moon}	Reduced moment of inertia of the Moon	0.3931 ± 0.0002	[Konopliv et al., 1998]	
ρ_{Moon}	Average density of the Moon	3.3437 ± 0.0016 g/cm^3	[Konopliv et al., 1998] Errors in the determination of the lunar mass ignored	
H_{cr}	thickness of the crust	$H_{cr} \in [0;50]$ km	Specified according to the seismic models [Nakamura 1983; Lognonné et al., 2003; Gagnepain-Beyneix et al. 2006; Khan et al., 2000; 2007], the crustal models [Wieczorek et al., 2006], and a series of preliminary calculations	
H_u	thickness of the upper mantle	$H_u \in [50;250]$ km		
H_m	thickness of the middle mantle	$H_m \in [250;650]$ km		
H_l	thickness of the lower mantle	$H_l \in [650;R_{Moon} - R_{core}]$ km		
ρ_{cr}	crustal density	2.9 g/cm^3		
Crustal composition	CFMAS system, wt % %	$Al_2O_3 = 25\%$, $CaO = 16.5\%$, $MgO = 7\%$, $FeO = 6.5\%$, $SiO_2 = 45.5\%$;	[Taylor, 1982]	
$T_k (k = u, m, l)$	Temperature in the mantle zones	$T_u = 600°C$ $T_m = 900°C$ $T_l = 1200°C$	Specified according to the models [Kuskov and Kronrod, 1998a; Kuskov and Kronrod, 2009]	

		Constraints on the output parameters of the models		
Model	Model	Mass	Balance of main oxides (6)	Seismic velocities in the upper and the middle mantle	Similar concentrations in the upper and the lower mantle
MI	+	+	+	−	−
MIS	+	+	+	+	−
MISC	+	+	+	+	+

the present work, the temperature was specified to be 600°C at a depth of 150 km, 900°C at 500 km, and 1200°C at 1000 km, according to the models [Kuskov and Kronrod, 1998a; Kuskov and Kronrod, 2009].

The depth distribution of pressure in the lunar interiors is determined according to the formula for the model with a constant density:

$$P = P_o\{1 - [(R - H)/R]^2\}, \tag{3}$$

where $P_o = 47.1$ kbar is the pressure in the center of the Moon, $R = 1738$ km, and H is depth.

3. THE THERMODYNAMICAL APPROACH

The equilibrium phase assemblages, velocities, and density of the lunar mantle are calculated using the THERMOSEISM database [Kuskov, 1997; Kuskov and Kronrod, 2001], which incorporates mutually consistent thermodynamic parameters (enthalpy, entropy, heat capacity, Grüneisen parameter, thermal expansion, bulk and shear moduli for minerals) and the mixing parameters of solid solutions. The CFMAS system includes the following solid solution phases:

plagioclase, ferromagnesian olivine, and spinel; pyrope−almandine− grossular garnet; and orthopyroxene and clinopyroxene, the 5- and 6-component solid solutions. The chemical composition of phases and their proportions are found by the method of the Gibbs free energy minimization. The equation of state (EOS) for minerals is calculated in terms of the quasi-harmonic Mie−Grüneisen−Debye approximation [Kuskov et al., 2006]. It yields the density and isotropic velocities $V_{P,S}(P, T, X)$ of the phase assemblage, which depend on the chemical and phase composition of the rock.

The P- and S velocities of the equilibrium phase assemblage $V_{P,S}(P, T, x)$, which take into account the effects of anharmonicity and phase transitions and are frequency independent, are calculated according to the formulas

$$V_P^2 = \frac{K_S + 4/3G}{\rho}, \quad V_S^2 = \frac{G}{\rho}, \tag{4}$$

where the bulk modulus (K_S) and density (ρ) of the phase assemblage are found from the equation of state.

The shear modulus is assumed to be linearly dependent on temperature and pressure.

Elastic moduli are calculated using the Voigt–Reuss–Hill approximation, which is commonly used in geophysical applications. Due to the extremely high G factor of the dry lunar interior, which exceeds the terrestrial value by an order of magnitude, the effects of anelasticity can be disregarded as their contribution is small compared to other model errors [Khan et al., 2007, Kronrod and Kuskov, 2007].

4. MODEL OF THE MOON AND METHOD OF SOLUTION

4.1. The Model

According to the seismic data, we assume in the models of the internal lunar structure that the Moon is composed of five spherical shells: the crust, the three-layer (upper, middle, and lower) mantle, and the iron sulfide core whose size is determined in the course of the solution. The following parameters were used: crustal thickness of 50 km, the upper mantle extending from 50 to 250 km, the middle mantle extending from 250 to 625 km, and the lower mantle extending from a depth of 625 km to the boundary with the core. The depths of the boundaries were specified according to the seismic models [Nakamura, 1983; Lognonné et al., 2003; Gagnepain-Beyneix et al. 2006; Khan et al., 2000; 2007] and the series of preliminary calculations on studying the influence of the thickness of the crust, the upper mantle, and the middle mantle on the output model parameters. Whatever the determination accuracy of these layers is, the depths of their boundaries provide an important factual frame for petrological interpretation. In this connection, we note that the topology of seismic profiles is naturally imprinted in the petrological models of the lunar interiors inferred from these seismic data.

Each of the three layers composing the mantle is adopted to have its own particular composition; however, within each zone the material is assumed to be practically homogeneous with a low gradient in chemical composition and a slightly varying density. Abrupt changes in the composition are only allowed to occur at the geophysical boundaries [Kronrod and Kuskov, 1997; Kuskov and Kronrod, 1998a]. Due to the lack of information and in order to simplify the procedure of the calculations, the densities (ρ_i) and the concentrations of the oxides (C_i = MgO, FeO, Al$_2$O$_3$, CaO, SiO$_2$) in each ith zone of the mantle are assumed to be constant throughout the whole depth interval and to satisfy a natural condition of no density inversion on the boundaries of the zones:

$$\partial\rho/\partial H > 0. \qquad (5)$$

The chemical composition of each zone of the mantle is assumed to be frozen and equal to the values in some average points of the mantle section (150 km, 500 km, and 1000 km in the upper, the middle, and the
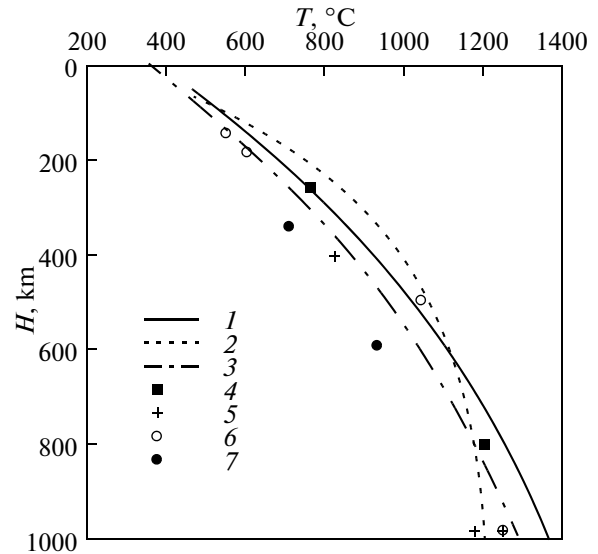

Fig. 2. Temperature distribution models in the lunar mantle. *1* according to Kuskov and Kronrod [1998a, model 1]; *2* according to Kuskov and Kronrod [1998a, model 2]; *3* according to Kuskov and Kronrod [2009]; *4* according to Hood and Zuber [2000]; *5* according to Gagnepain-Beyneix et al. [2006]; *6* according to Khan et al. [2006a; 2006b]; *7* according to Lognonné et al., [2003]. The temperature for the models [Khan et al., 2006a; 2006b] and [Gagnepain-Beyneix et al., 2006] was estimated from the graphs, as numerical values are not cited in these works.

lower mantle, respectively). The density and the seismic velocities are determined at the same points as the composition. It is postulated that the concentrations of Al$_2$O$_3$ and CaO in the initial lunar material are linked by the relation CaO = KAl$_2$O$_3$, where K is ~0.8 [Ringwood and Essene, 1970].

The compositional differentiation of the outer shells of the mantle relative to the lower (primary) mantle is inferred from the balance conservation conditions for the oxides in the CFMAS system and the geophysical constraints. The models of the magma ocean in such a formulation were considered in our previous work [Kuskov and Kronrod, 1998b].

The balance of the rock-forming oxide concentrations for the model of differentiation of the initially chemically homogeneous Moon into the crust, the upper, and the middle mantle is characterized by the following conditions:

$$\delta_C = C_l - (\rho_{cr}v_{cr}C_{cr} + \rho_m v_m C_m$$

$$+ \rho_u v_u C_u)/(\rho_{cr}v_{cr} + \rho_m v_m + \rho_u v_u) < \delta_{max}, \qquad (6)$$

(C = MgO, FeO, Al$_2$O$_3$, CaO, SiO$_2$). Here, ρ, v, and C are, respectively, the density, the volume, and the oxide concentrations (wt %). The indices $cr, u, m,$ and l correspond to the crust, the upper, the middle, and the lower mantle, respectively. δ_C describe the deviations from the balance equations, and δ_{max} is the maximum permissible deviations for the Cth oxide. For example,

all δ_C being zero means that the chemical composition of the modern lower mantle should be equal to the composition of the uniformly mixed overlying shells.

4.2. Method of Calculation

The optimization procedure for solving the inverse problem of inferring the chemical and mineral composition and the radius of the lunar core from the set of geophysical constraints is described in [Kronrod and Kuskov, 1997; Kuskov and Kronrod, 1998a; Kuskov et al., 2002]. In the present work, we apply Monte-Carlo sampling over a uniform distribution [Sambridge and Mosegaard, 2002]) to solve the problem of the chemical differentiation of the Moon. This method allows one to analyze all possible domains of the solution for a multi-parametric problem with all kinds of constraints imposed and to yield a full range of all possible solutions instead of a single one, which is optimal in a certain sense, as has been done in the previous works. Thereby, we can find the probable distributions of the concentration profiles for the rock-forming oxides and the seismic velocities in three mantle reservoirs and can also estimate the mean values and deviations of the obtained distributions.

The problem is formulated as follows: we find the values of seismic velocities, density, and oxide concentrations in the mantle reservoirs such that they obey the balance conditions (6) and the conservation equations for the mass M^o and the moment of inertia I^o of the Moon:

$$M^o = \frac{4}{3}\pi \sum_{i=1}^{L} \rho_i \left(R_i^3 - R_{i+1}^3 \right) + \delta M^o, \qquad (7)$$

$$I^o = \frac{8}{15}\pi \sum_{i=1}^{L} \rho_i \left(R_i^5 - R_{i+1}^5 \right) + \delta I^o. \qquad (8)$$

as well as the no-inversion conditions for density (5) and additional constraints on seismic velocities and concentrations in the three-mantle zones of the Moon. Here, ρ_i is the density of the ith layer, R_{i+1}, and R_i are the minimum and the maximum radii of the ith layer, δM^o, and δI^o are the errors in the determination of the mass and the moment of inertia of a satellite, and L is the number of layers in the model of the Moon. In the case considered, $L = 5$. In the calculations, the modeled moment of inertia was allowed to deviate from the experimental value within the experimental accuracy range. The errors in the determination of the lunar mass were disregarded as they are fairly small compared to other errors. The dimensionless moment of inertia ($I^* = I^o/M^oR^2 = 0.3931 \pm 0.0002I$), the average density ($\rho^* = 3.3437 \pm 0.0016$ g/cm^3), and the lunar radius ($R^* = 1738$ km) were specified following [Konopliv et al., 1998].

While solving the multi-parametric problem of retrieval of the chemical composition and physical properties in each mantle zone and the size of the lunar core, we sought a solution that would satisfy (5), (7), and (8), meet the constraints on the concentrations and seismic velocities in various zones in the mantle, and ensure the fulfillment of balance equations (6):

$$Q = \sqrt{\frac{1}{5}\sum_{C} \delta_C^2},$$

$$C = \text{MgO, FeO, Al}_2\text{O}_3\text{, CaO, SiO}_2 \qquad (9)$$

$Q < Q_{\max}$.

The value $Q_{\max}$ reflects the deviation of the bulk composition of the undifferentiated lower mantle from the average composition of the crust + upper mantle + middle mantle system.

5. THE RESULTS OF CALCULATIONS

The bulk composition, the size of a core, and the concentrations of the main oxides in the models of the Moon depend on the constraints imposed on the sought solution. Below, we consider lunar models with various constraints on the velocities and the main oxide concentrations in the mantle of the Moon.

5.1. Lunar Models Constrained by the Mass, the Moment of Inertia, and the Seismic Velocities in the Upper and Middle Mantle (MIS)

The input data for this type of models, which will be referred to as MIS models, include the mass and the moment of inertia of the Moon and the seismic information. As the seismic profiles show great uncertainty in the lower mantle, the seismic models [Lognonné et al., 2003; Lognonné et al., 2005; Gagnepain-Beyneix et al., 2006] are only used at the depths of the upper and middle mantle, while the velocities in the lower mantle are inferred from the solution of the inverse problem.

In our calculations, the seismic velocities in the upper and middle mantle were bounded by the limits of the deviations of the mean values for the corresponding model (Table 1):

$$V_{j\max} > V_j > V_{j\min} \ (j = p, s). \qquad (10)$$

The solution of the inverse problem gives the geophysically and geochemically permissible distributions of velocity (Table 1, Figs. 3 and 4) and concentrations (Table 3, Fig. 3) in the mantle of the Moon and the size of the Fe-FeS lunar core (Fig. 5). Every pair of seismic velocities V_P and V_S, which fall within the interval of possible solutions shown in Fig. 3, meets all the constraints for the given type of models, including (7)−(9) and (10), although with a different deviation from the average experimental values of the moment of inertia, seismic velocities, and balance equations (9). In all the cases considered, the misfits between the calculated and the empirically estimated

Table 3. Concentrations of main oxides (wt %) in the zonal mantle of the Moon

Model	Zone	$Al_2O_3^*$	FeO*	MgO*	SiO_2^*
MI[1]	50–250 km	3.0 ± 1.1	8.9 ± 1.2	32 ± 1.7	54 ± 1.2
	250–625 km	4.6 ± 1.37	11.4 ± 1.7	35 ± 2.2	45.4 ± 3.5
	>625 km	5.8 ± 1.0	9.9 ± 1.1	30.6 ± 1.2	49 ± 1.5
MIS[2]	50–250 km	1.62 ± 0.43	11.4 ± 0.7	31.1 ± 0.9	54.6 ± 1
		1.9 ± 0.7	10.5 ± 1.1	34.6 ± 2.1	51.5 ± 2.1
	250–625 km	2.2 ± 0.5	13.9 ± 0.7	33.3 ± 1.7	48.9 ± 1.4
		2.7 ± 0.8	13.3 ± 1.2	31.1 ± 2.0	50.4 ± 1.9
	>625 km	4.1 ± 0.5	12.1 ± 0.5	29.5 ± 0.9	50.9 ± 0.6
		4.8 ± 0.65	11.4 ± 0.9	29.8 ± 1.2	49.5 ± 1.2
MISC[3]	50–250 km	1.6 ± 0.5	11.8 ± 0.5	31.4 ± 0.5	54.1 ± 1
	250–625 km	1.8 ± 0.6	12.2 ± 0.5	31.5 ± 0.5	53.2 ± 1.2
	>625 km	3.8 ± 0.5	11.7 ± 0.5	28.8 ± 0.5	52.6 ± 1.2

Notes: [1] MI model, constraints on the mass and the moment of inertia of the Moon

[2] MIS model, constraints on the mass, the moment of inertia, and the seismic velocities in the upper and the middle mantle. The values presented in the upper lines are the constraints according to the model of Gagnepain-Beyneix et al. [2006], and those in the lower lines, according to the model in [Lognonné et al., 2005].

[3] MISC model, constraints on the mass, the moment of inertia, and the seismic velocities in the upper and the middle mantle according to the model of Gagnepain-Beyneix et al. [2006] plus the condition of similar concentrations in the upper and the middle mantle.

[1,2,3] Concentrations of the main oxides in the lower mantle correspond to the bulk composition of the silicate portion of the Moon (the crust plus the mantle). The values of concentrations with an asterisk in the upper index (*) and the corresponding errors in the present models are the mean values and the standard deviations calculated assuming normal distributions in the frequency histograms. Concentrations of CaO are equal to $0.8CAl_2O_3$.

values of the moment of inertia and seismic velocities (with the velocity constraints for the mantle zones) lie within the errors of the experimentally determined parameters. At the same time, the higher frequencies in the histograms of the frequency distribution correspond to the solutions with smaller deviations from the average experimental values. The misfit in the lunar mass determination is zero. In the estimation of the mean values of the obtained distributions, e.g., of seismic velocities shown in Fig. 3 and their deviations, the distribution was assumed to be normal. The errors (Tables 1 and 3) do not include probable systematic errors caused by the uncertainties present in the input data and the assumptions adopted in the formulation of the problem and in the calculation of the physical parameters of the lunar interior. According to the statement of the problem, the concentrations of the main rock-forming oxides in the lower mantle correspond to the bulk composition of a silicate portion of the Moon within an accuracy of at most 0.3–0.5 wt % (Table 3).

The bulk composition of the lower mantle in wt % is the following: $Al_2O_3^* = 4.1, 4.8\%$; CaO* = 3.3, 3.8%; FeO* =12.1, 11.4%; MgO*=29.5, 29.8%; $SiO_2^* = 50.9$, 49.5%; MG*#81.3, MG*#82.3. Further in this sec-

tion, the first value corresponds to the model [Gagnepain-Beyneix et al., 2006], and the second, to the models [Lognonné et al., 2003; Lognonné, 2005]. The upper index (*) is assigned to the mean values of the calculated parameters. It can be seen that the chemical composition of the silicate Moon in the model constrained according to [Gagnepain-Beyneix et al., 2006] features somewhat smaller mean concentrations of Al_2O_3 and higher concentrations of FeO compared to the model following [Lognonné et al., 2003; Lognonné, 2005]. The calculations showed that the limits of permissible concentrations (wt %) in the model [Gagnepain-Beyneix et al., 2006] are appreciably narrower, measuring 3–5.5% Al_2O_3, 2.4–4% CaO, 10.5–13.5% FeO, 28–31.5% MgO, and 49–52% SiO_2. The limits of permissible values are understood as the intervals of the sought parameters that provide a solution of the inverse problem that meets all the constraints posed.

The mean radius of the core of the Moon is $R_{core}^* = 340 \pm 30$ km, 380 ± 55 km (Fig. 5). These results quite well correlate with the estimates $R_{core} \approx 350$ km presented in [Kuskov and Kronrod, 1998a; Khan et al., 2007]. The distribution of the permissible values of density for the seismic model [Gagnepain-Beyneix
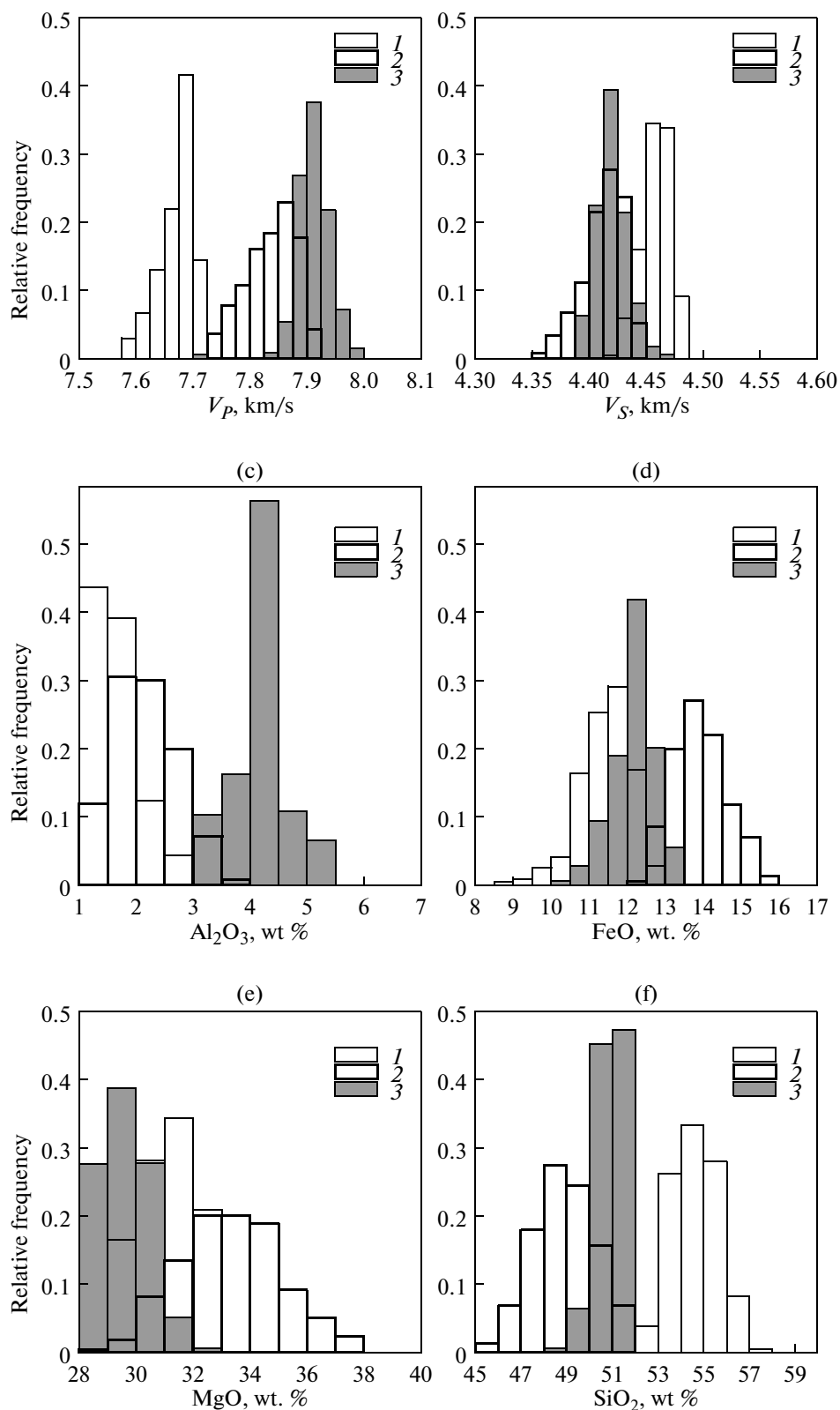
Fig. 3. Seismic velocities and concentrations of main oxides in the mantle of the Moon for MIS model constrained by the mass, the moment of inertia, and the seismic velocities in the upper and the middle mantle, according to [Gagnepain-Beyneix et al., 2006]. *1, 2, 3* are the upper, the middle, and the lower mantle, respectively. (a) *P* waves; (b) *S* waves; (c) Al_2O_3; (d) FeO; (e) MgO; (f) SiO_2.
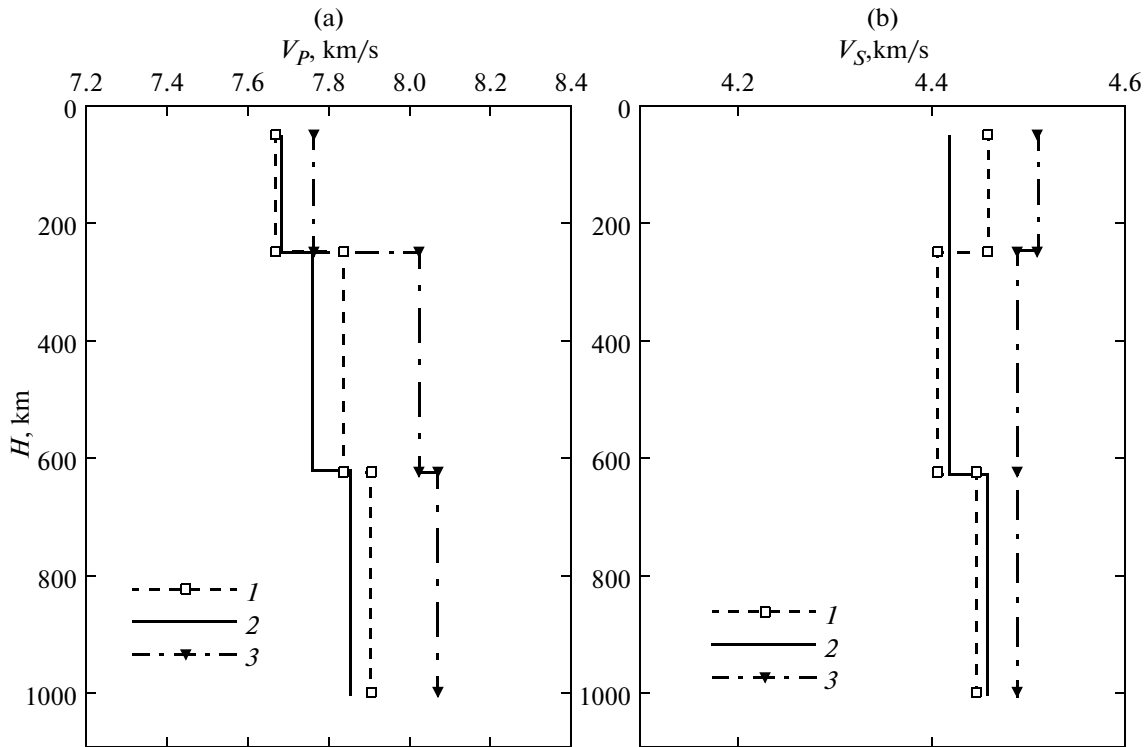
Fig.4. Velocity profiles (mean values of the frequency distributions) for *P* waves (a) and *S* waves (b) in the lunar mantle. *1* MIS model with the constraints on the mass, the moment of inertia, and the seismic velocities in the upper and the middle mantle, according to [Gagnepain-Beyneix et al., 2006]; *2* MIS model plus the conditions of equal concentrations in the upper and the middle mantle (MISC model); *3* MI model with the constraints on the mass and the moment of inertia.

et al., 2006] are shown in Fig. 6; the densities in the upper, the middle, and the lower mantle are $\rho_u^* = 3.311 \, g/cm^3$, $\rho_m^* = 3.375 \, g/cm^3$, and $\rho_l^* = 3.386 \, g/cm^3$, respectively.

The seismic velocities in the lower mantle are of particular interest for us, as they have not been bounded by any constraints. We obtained the following estimates: $V_P^* = 7.88-7.94, 7.92-8.02 \, km/s$; $V_S^* = 4.40-4.44, 4.48-4.54 \, km/s$ (Table 1, Fig. 4). These estimates for the *P* velocities are close to the mean values of $7.90 \pm 0.30 \, km/s$ reported in [Lognonné et al., 2003]; and those for the *S* velocities are close to the mean values of $4.50 \pm 0.10 \, km/s$ presented in [Gagnepain-Beyneix et al., 2006].

5.2. Lunar Models Constrained by the Mass, the Moment of Inertia, the Seismic Velocity, and the Concentrations in the Upper and Middle Mantle (MISC)

The investigations of the seismic structure of the lunar interior suggest a zonal constitution of the Moon with a seismic boundary estimated at a depth of 500–700 km. The presence of a seismic boundary at a depth of about 300 km is interpreted differently by scientists. Although this boundary can be identified in the aver-

age values in the models [Nakamura, 1983; Gagnepain-Beyneix et al., 2006], the models [Goins et al., 1981; Lognonné, 2005; Khan et al., 2007] do not provide an explicitly distinguishable boundary between the upper and the middle mantle. In this section of the paper, we explore the possibility of constructing models of the Moon in which the chemical compositions in the upper and the middle mantle are practically similar to each other and the seismic velocities in these layers of the mantle are constrained according to the seismic models. As shown in [Kuskov, 1997; Kuskov and Kronrod, 1998a], this zone is void of phase transitions which might be responsible for the stepwise changes in the velocity and density. Therefore, in such models, the differences in the velocities in the upper and the middle mantle can only be driven by *P-T* conditions, and the phase interface at a depth of 250–300 km is improbable. It can be seen from Fig. 3 that there are common domains for the concentrations of the main oxides in the upper and the middle mantle, which indicates that the solutions without a chemical boundary between the upper and the middle mantle are very likely. Let us now attempt constructing the model of the Moon, which would meet the conditions for the mass and the moment of inertia, the balance equations, and the seismic constraints according to the model [Gagnepain-Beyneix et al., 2006], as well as
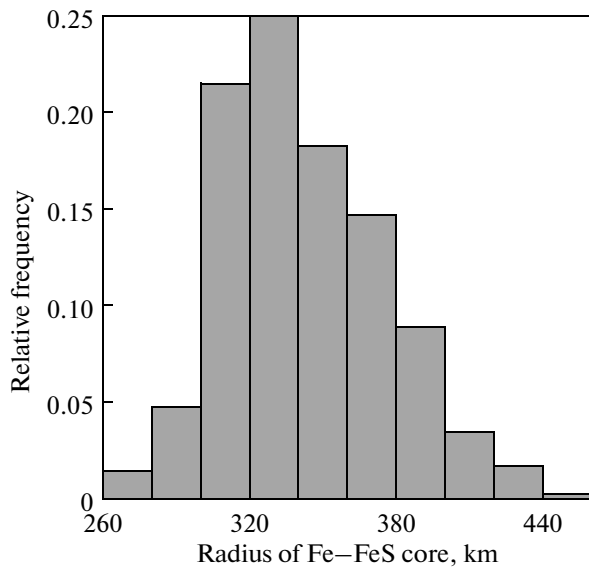
Fig.5. The radius of Fe–FeS core. MIS model with the constraints on the mass, the moment of inertia, and the seismic velocities in the upper and the middle mantle, according to [Gagnepain-Beyneix et al., 2006].

the conditions of similar concentrations in the upper (C_u) and the middle (C_m) mantle, the MISC model:

$$|C_u - C_m| < 0.5 \text{ wt } \%$$
$$(C = Al_2O_3, CaO, MgO, FeO, SiO_2).$$
(11)

Having solved the inverse problem, we obtain a range of models which meet all the conditions stated. The distributions of density, concentrations, and velocities are found for all mantle zones. This indicates that the models of a differentiated Moon with an almost homogeneous chemical composition up to the top of the lower mantle are possible. The obtained distributions of the concentrations and velocities in the mantle are close to the models discussed in Section 5.1 (Tables 1 and 3, and Figs. 4 and 7). The velocity profiles are similar to those obtained in Section 5.1. Due to the additional constraints on the concentrations, the limits of permissible seismic velocities in the lower mantle in the MISC model are significantly narrower (7.8–7.92 km/s for V_P and 4.42–4.5 km/s for V_S). The P velocities in the upper and middle mantle correspond to the model of Gagnepain-Beyneix et al. [2006], and in the lower mantle, to the model of Lognonné et al. [2003]. The S velocities in all zones are well correlated with the model [Gagnepain-Beyneix et al., 2006] (Table 1, Fig. 4).

5.3. Models of the Moon Constrained by the Mass and the Moment of Inertia (MI)

We consider the constraints on the seismic velocities and chemical composition of the lunar mantle, which follow from the conditions imposed only on the
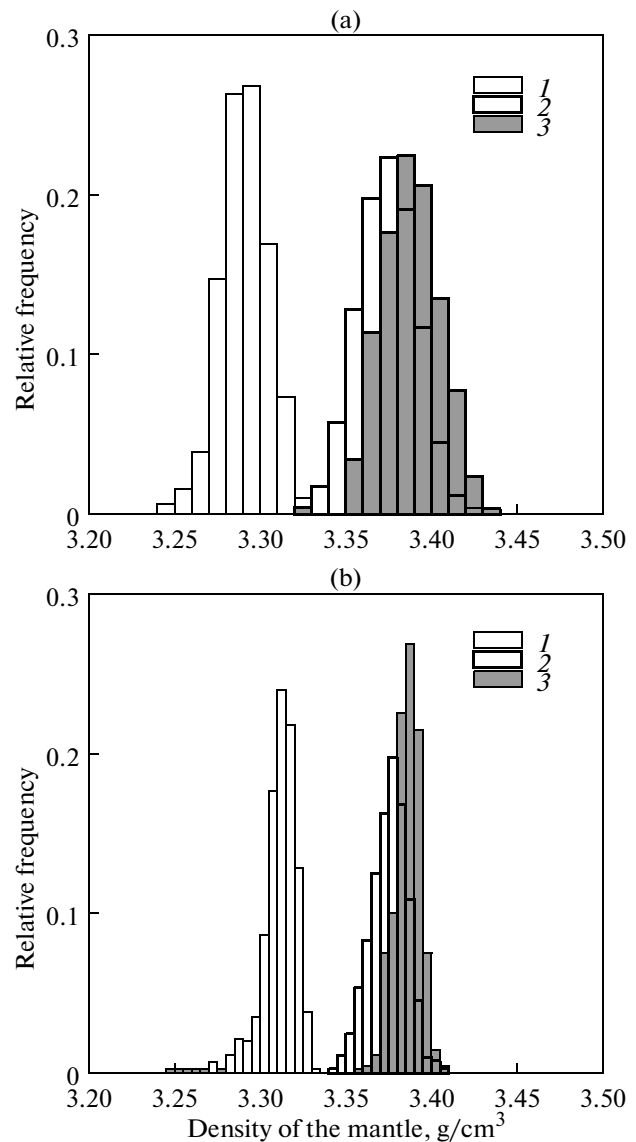

Fig. 6. The density in the lunar mantle. (a) MI model with the constraints on the mass and the moment of inertia; (b) MIS model with the constraints on the mass, the moment of inertia, and the seismic velocities, according to [Gagnepain-Beyneix et al., 2006]. *1, 2, 3* are the upper, the middle, and the lower mantle, respectively.

moment of inertia, the mass (7) and (8), and the balance equations (6) (MI model). The mean velocities agree well with the model [Lognonné et al., 2003] in both V_P and V_S in the upper mantle and in V_S in the middle mantle, and with the model [Gagnepain-Beyneix et al., 2006] in V_P and V_S in the middle and the lower mantle (Table 1, Fig. 4). Despite the large intervals of permissible concentrations, the bulk composition of the silicate Moon is estimated with an error as small as about 1 wt %: $Al_2O_3^* = 5.8 \pm 1\%$, $FeO^* = 9.9 \pm 1.1\%$, $MgO^* = 30.6 \pm 1.2\%$, $SiO_2^* = 49 \pm 1.5\%$,
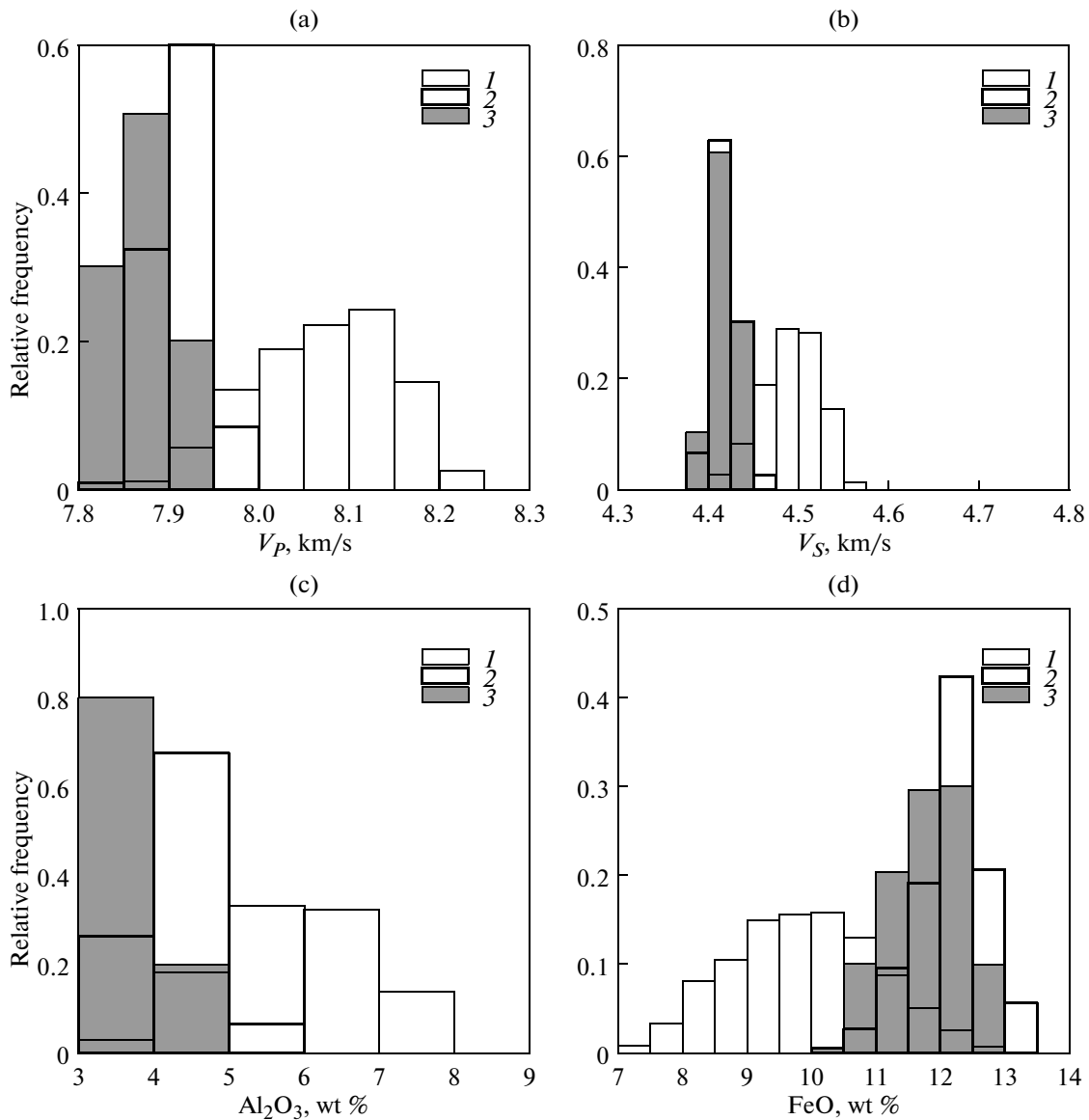
Fig. 7. Frequency distributions of seismic velocities and concemtrations in the lower mantle of the Moon for different models. (a) S velocities; (b) P velocities; (c) Al_2O_3; (d) FeO. (*1*) MI model with the constraints on the mass and the moment of inertia; (*2*) MIS model with the constraints on the mass, the moment of inertia, and the seismic velocities, according to [Gagnepain-Beyneix et al., 2006]; (*3*) MISC model with the constraints on the mass, the moment of inertia, and the seismic velocities, according to [Gagnepain-Beyneix et al., 2006], plus the conditions of equal concentrations in the upper and the lower mantle. Concentrations of the main oxides in the lower mantle correspond to the bulk composition of the silicate portion of the Moon (the mantle plus the crust).

MG*#84.5, Table 3 and Fig. 7. It is worth noting that this chemical composition of the Moon well agrees with the models of Kuskov [1997] and Kuskov and Kronrod [1998a], although the MI model does not invoke seismic information.

The distributions of the permissible values of density for different mantle zones are shown in Fig. 6. The mean values for the upper, the middle, and the lower mantle are, respectively, $\rho_u^* = 3.291$ g/cm³, $\rho_m^* = 3.375$ g/cm³, and $\rho_l^* = 3.389$ g/cm³, which is very

close to the MIS model. The mean radius of the lunar core is $R^* = 375 \pm 55$ km.

6. RESULTS AND DISCUSSION

6.1. Basic Model Assumptions

The interpretation of the results of inversion largely depends on the assumptions adopted in the formulation of the problem, on the errors in the input data, and on the uncertainties in the solution. The basic assumptions in the model of Magma Ocean are the

following. The outer lunar shells undergo melting, which is followed by the subsequent differentiation of the Moon into the crust, the upper mantle, and the middle mantle. The Moon is assumed to be a perfect sphere with a radially symmetric multilayer structure. The asymmetry of the Moon is ignored. The thickness, the density, and the chemical composition of the crust are specified according to the data provided by the Apollo mission and subsequent geophysical investigations. The density and the chemical composition of each mantle layer (the upper, the middle, and the lower mantle) are assumed to be constant throughout the entire interval of corresponding depths; the same applies to the core as well. The local seismic information and other data inferred from the samples taken at the Apollo landing sites are assumed to apply for the global Moon. The temperature distribution in the lunar interiors is specified according to the models based on the seismic information, which has significant uncertainties at a depth below 500 km [Kuskov and Kronrod, 2009]. Each of the listed assumptions contains errors that affect the output results, which should be taken into account when interpreting the results of modeling. For example, the mass and the moment of inertia of the Moon can be estimated with at least the same error as that in the calculation of density.

In terms of the statement of the problem, the present work has many aspects in common with our previous investigations [Kronrod and Kuskov, 1997; Kuskov and Kronrod, 1998a; 1998b]. The main differences are the method of solution and the range of models to be studied. The approach applied in the present work offers a remarkable advantage: it yields the entire range of all possible solutions instead of a single optimal solution, as provided in our previous works. This technique ensures a more adequate and reasonable evaluation of the possible lunar models. By applying the advanced numerical methods and by using the modern data on seismic velocities, we were able to outline the ranges of geophysically and geochemically permissible seismic velocities and concentrations of the main rock-forming oxides in the lunar mantle. It is notable that the mean values of the studied parameters in the histograms of the frequency distribution correspond, in some sense, to the optimum solutions, i.e., to those best fitting all the constraints imposed on the model under consideration. In terms of qualitative assessment, the increased number of successful solutions (the variants that satisfy all posed constraints) indicates their smaller deviation from the optimal solution. At the same time, it is very likely that there are some additional geochemical and thermophysical constraints inherent in the nature of the Moon which do not correlate to the mean values of the inferred distributions. The additional constraints not considered in our present work may shift the mean values of the distributions relative to the estimates we obtained here. However, in any case, the values of the sought parameters should fall within the limits of the obtained distributions (Figs. 3, 5, and 7). These considerations apply for all sought parameters in all the models discussed above.

6.2. Effects of the Variations in the Input Parameters

The effects, which the variations in the input parameters relative to the reference model (see Table 2) produce in the bulk composition of the Moon and in the seismic P and S velocities in the lower mantle, are estimated in Table 4. The numerical experiments for the model with seismic constraints according to [Gagnepain-Beyneix et al., 2006] have shown that temperature variations alone ($\Delta T \pm 50°C$) or variations in the positions of the boundaries between the upper–middle mantle ($\Delta H_{cr-u} = +50$ km) and the middle–lower mantle (($\Delta H_{m-l} = \pm 125$ km) within the indicated limits only slightly affect the results. The total effect of variations in crustal thickness, crustal density, and the depth of the seismic boundaries on the bulk composition of the silicate Moon and on the seismic velocities in the lower mantle is negligible, as the variations in the different input parameters cause opposite-sign (mutually annihilating) effects in the calculation. The main effects of the increasing concentration of Al_2O_3 in the crust up to 30 wt % are the ~0.5 wt % increase in Al_2O_3 in the bulk composition and the ~0.6 wt % decrease in SiO_2 relative to the reference solution (Table 4). The variations in the mean concentrations of the main oxides in the lower mantle relative to the reference solution, which are caused by the simultaneous changes in all four input parameters, are at most 1 wt %. All this indicates that the obtained solutions are rather conservative to relatively small variations in the input parameters of the models.

6.3. MI Models and the Symmetry of the Internal Structure of the Moon

The MI model, the coarsest one, is based on the information on the moment of inertia and the mass of the Moon and the balance equations (6). No constraints are imposed on the profiles of seismic velocities. By comparing the mean seismic velocities and bulk silicate Moon in the MI model with the geophysical and geochemical models, we see that the constraints on the mass and the moment of inertia alone provide quite reasonable results (Fig. 4, Tables 1 and 3).

To date, there is no reliable evidence for the full central symmetry of the internal constitution of the Moon. Strictly speaking, the seismic velocities in the lunar interiors are determined only locally, at the Apollo landing sites. In the majority of the existing models of the internal lunar composition, the local seismic data provided by the Apollo mission are extended onto the whole Moon. Wieczorek et al. [2006] in their review discuss a model with a seismic boundary at a depth of 500 km, which has been formed

Table 4. Effects produced in the lower mantle seismic velocities and in the bulk composition of the silicate portion of the Moon by the variations in the input parameters of the model relative to the reference[1] model (see Table 2)

Variation in the model parameter	Velocities in the lower mantle		Bulk composition, wt %			
	V_P, km/s	V_S, km/s	MgO	FeO	Al_2O_3	SiO_2
H^2_{cr-u} + 125 km	+0.004	−0.004	+0.08	+0.13	−0.14	−0.03
H_{m-l} − 125 km	+0.017	+0.013	−0.46	−0.48	+0.38	+0.25
H^3_{cr-u} + 10 km	+0.029	+0.003	−0.160	+0.26	+0.45	−0.91
ρ^4_{cr} + 0.1 g/cm³	−0.005	+0.009	−0.21	−0.75	−0.02	+1.0
$Al_2O^5_{3cr}$ +5 wt %	+0.034	+0.009	−0.05	−0.18	+0.45	−0.56
H_{m-l} + 125 km H_{cr-u} + 10 km ρ_{cr} + 0.1 g/cm³	+0.018	+0.007	−0.05	−0.21	+0.23	−0.15
H_{m-l} + 125 km H_{cr-u} + 10 km ρ_{cr} + 0.1 g/cm³ $Al_2O_{3\,cr}$ + 5 wt %	+0.052	+0.027	−0.15	−0.28	+0.72	−0.87

Notes: [1] Reference model: Al_2O_{3cr} = 25 wt %, ρ_{cr} = 2.9 g/cm³, H_{cr-u} = 50 km; H_{m-l} = 625 km.
[2] H_{m-l} is the depth of the boundary between the middle and the lower mantle.
[3] H_{cr-u} is the depth of the boundary between the crust and the upper mantleÿ.
[4] ρ_{cr} is the crustal density
[5] $Al_2O_{3\,cr}$ is the concentration of Al_2O_3 in the crust

as a result of heating followed by a subsequent melting and differentiation exactly in the region of the Oceanus Procellarum. In this case, the known seismic models should only apply for this particular region. To elucidate the issue, one may refer to the results provided by the MI model. As these models were constructed without seismic constraints, the resulting distributions of the velocities and concentrations correspond to the radially symmetric models of lunar interiors. The fact that the model estimates of the mean seismic velocities are close to the experimental values measured by the Apollo seismographs can serve as evidence in favor of the radial seismic symmetry of the Moon.

In our calculations, the mean values of V_P and V_S in the MI model practically coincide with those for the model of Lognonné et al. [2003] in the upper mantle and with the results of Gagnepain-Beyneix et al. [2006] in the lower mantle. Moreover, the bulk composition of the silicate portion of the Moon is close to the results obtained in [Kuskov, 1997; Kuskov and Kronrod, 1998a; 1998b] (Table 5). In [Khan et al., 2006b], the chemical composition of the Moon is retrieved from the electromagnetic data, the moment of inertia, and the mass. The results on the bulk composition are similar to our estimates for the MI model; both models have the mean magnesium number MG#84. This effect is probably due to the fact that the

mass and the moment of inertia of the Moon are the dominant constraints on the density distributions in the lunar interiors and, as a consequence, on the mineral composition and seismic velocities. The additional balance conditions set for the chemical composition in our models, or the electromagnetic constraints [Khan et al., 2006b] somewhat narrow down the intervals of permissible values of the sought parameters.

Therefore, based on the results obtained for the MI model (the mean seismic velocities and concentrations of main oxides in the lunar mantle), we may qualitatively conclude that the seismic models and the zonal structure of the Moon inferred from the local measurements by the Apollo mission apply for the global Moon as well.

6.4. MIS Models

The MIS model, which follows the MI models in terms of complexity and is the basic model in terms of the statement of the problem, in addition to the moment of inertia and the mass of the Moon, uses information on seismic velocities in the upper and middle mantle. A comparison between these two models shows that the interval of permissible concentrations of the main oxides and the seismic velocities becomes considerably narrower as the degree of constraints on the models increases (Fig. 7). The permis-

sible ranges of seismic velocities for the lower mantle in the MIS model of 7.84−8 km/s for the P waves and 4.36−4.46 km/s for the S waves are noticeably narrower than in the seismic models presented in [Lognonné et al., 2003; Gagnepain-Beyneix et al., 2006]. The mean concentrations in the upper and the middle mantle for the MIS model are, generally, different.

The concentrations of $Al_2O_3^*$ and FeO^* in the upper mantle are lower, respectively, by 0.6−0.8%, and 1.9−3.4% than in the middle mantle (Fig.3, Table 3).

A hint of a correlation between the concentrations of Al_2O_3 and FeO is perceived in the lower mantle. The smallest concentrations of ~3% Al_2O_3 correspond to 11−13.5% FeO. For the highest concentrations of 5−5.5% Al_2O_3, the corresponding FeO concentrations are somewhat lower, ranging from 10.5−12.5%. The upper mantle is represented by the phase assemblage containing 2 mol % olivine + 93.8% orthopyroxene + 4.2% clinopyroxene. Orthopyroxene also prevails in the middle mantle (62 mol %); the other phases here are olivine (30%), clinopyroxene (5.8%), and garnet (1.6%). These phase compositions were calculated for the mean concentrations of the main oxides (Table 3).

The lower mantle is more abundant in Al_2O_3 and CaO compared to the upper and the lower mantle. This manifests itself in higher concentrations of garnet (3.9 mol %) and clinopyroxene (11.7 mol %); the molar concentrations of olivine and orthopyroxene are 13.7 and 70.7 mol %, respectively. The middle mantle is to some extent enriched in FeO (~ 2 wt %) compared to the lower mantle (Fig. 3), which qualitatively agrees with our previous estimates [Kronrod and Kuskov, 1997; Kuskov and Kronrod, 1998a; 1998b]. In contrast to the model of Nakamura [1983] (Fig. 1), our present calculations have not revealed any distinct inversion of seismic velocities in the middle mantle (Fig. 4). Solutions with the inversion of velocity in the middle mantle are unlikely, although possible. Our estimates of the mean S velocities in the lower mantle ($V_S^* = 4.42 \pm 0.014$ km/s) almost coincide with the mean values in the model [Gagnepain-Beyneix et al., 2006], and the P velocities $V_P^* = 7.91 \pm 0.025$ km/s are close to the results presented in [Lognonné et al., 2003].

According to our calculations, the seismic velocity ratio V_P^*/V_S^* in the lower mantle is 1.77−1.79. To compare with, $V_P/V_S = 1.81$ in the model [Gagnepain-Beyneix et al., 2006], 1.88 in the model [Lognonné et al., 2003], and 1.80−1.82 in the model [Kuskov and Kronrod, 2009]. Our estimates based on the histograms of frequency distribution show that the permissible ranges of seismic velocities in the lower mantle are 7.82−8.08 km/s for P waves and 4.37−4.5 km/s for S waves. From the comparison presented above it follows that the P velocities in the model [Gagnepain-Beyneix et al., 2006] (8.15 ± 0.23 km/s) and S veloci-

ties in the model [Lognonné et al., 2003] (4.20 ± 0.30 km/s) meet our estimates, with mutual errors taken into account.

6.5. MISC Models

We have also analyzed the feasibility of the models with a nearly chemically uniform upper and middle mantle (the chemical composition is practically constant from the crust to the top of the lower mantle) and seismic constraints of the MISC models (Figs. 4 and 7, Tables 1 and 3). In terms of the velocities and concentrations of the main oxides in the lower and upper mantle, the MISC models are close to the MIS models. It is reasonable to compare the calculations for the MISC model with the model presented in [Khan et al., 2007], where the chemical composition shown in the graphs does not exhibit any variations up to a depth of 600−700 km. The difference in the mean concentrations in the histograms of distribution for Al_2O_3 and FeO between our models and the model by Khan et al. [2007] is insignificant. The magnesium numbers are also almost similar: Mg#81 in our model and Mg#82 in the model [Khan et al., 2007]. One should not expect our models to fully coincide with the results by Khan et al. [2007], as in the present work, the geophysical constraints are strengthened by the conditions imposed on the balance of the main oxides.

It is significant that within the given model class, the concentrations of the main oxides, except for Al_2O_3 and CaO, slightly vary with depth throughout the entire mantle including its lower layers. In contrast to [Khan et al., 2007], we have obtained the quantitative estimates for the seismic velocities in the lower mantle, which coincide with the values reported in [Lognonné et al., 2003] in terms of mean P velocities and with the results of [Gagnepain-Beyneix et al., 2006] in terms of mean S velocities (Table 1).

6.6. Chemical (Concentration) Boundaries in the Mantle

According to the modern geophysical constraints, models of the Moon that are chemically differentiated into the upper and the lower mantle and those with uniform composition up to the lower mantle are both possible. The chemical boundary at a depth of 500−750 km is present in all our calculations. We have estimated the crustal density and the depth of the chemical boundaries in the lunar shells from the relative frequency of the successful solutions for the MIS models. The studied parameters varied within the following limits: $2.9 < \rho_{cr} < 3.1$ g/cm³, $40 < H_{cr-u} < 60$ km, $250 < H_{u-m} < 300$ km, and $500 < H_{m-l} < 750$ km. Here, H_{cr-u}, H_{u-m}, and H_{m-l}, are the depths of the boundaries between the crust and the upper mantle, the upper mantle and the middle mantle, and the middle mantle and the lower mantle, respectively. Our results $\rho_{cr} = 2.9$ g/cm³, $H_{cr-u} = 50$ km, $H_{u-m} = 250$ km, and $H_{m-l} =$

Table 5. Model compositions for the silicate portions (the crust plus the mantle) of the Earth and the Moon (wt %)

Source of information	SiO$_2$	FeO	MgO	CaO	Al$_2$O$_3$	MG#
the Earth						
[Ringwood, 1979]	45.9	8.1	38.8	3.2	4.0	89.5
[Taylor, 1982]	50.1	8.0	35.3	2.9	3.7	88.8
[McDonough, Sun, 1995]	45.5	8.2	38.2	3.6	4.5	89.3
the Moon						
[Ringwood, 1979]	45.1	14.1	32.9	3.7	4.2	80.6
[Jones, Delano, 1989]	46.1	12.6	35.0	2.8	3.5	83
[O'Neill, 1991]	44.9	12.5	35.3	3.3	4.0	83
[Wänke, Dreibus, 1986]	45.9	13.1	32.6	3.8	4.6	81.6
[Taylor, 1982]	43.9	13.1	32.3	4.6	6.1	81.5
[Galimov, 2004]	43.4	13 + Fe in the core	32	10.8 (sum CaO + Al$_2$O$_3$)	81.5	
[Lognonné et al., 2003]	53.5	13.3	21.9	4.9	6.4	74.6
[Khan et al., 2007]	46.1	12.2	34	3.6	4.1	82
[Kuskov, 1997]	49.9	10.8	27.5	4.9	6.9	82
[Kuskov, Kronrod, 1998a]						
Model 1	50.0	10.4	28.5	4.8	6.3	83
Model 2	48.5	11.7	29.6	4.3	5.9	82
Present work, MI model[1]	49 ± 1.5	9.9 ± 1.1	30.6 ± 1.2	4.7 ± 0.8	5.8 ± 1	84.5
Present work, MIS model[2]	50.9 ± 0.6	12.1 ± 0.5	29.5 ± 0.9	3.4 ± 0.4	4.1 ± 0.5	81.3
	49.7 ± 1.2	11.6 ± 0.9	30.0 ± 1.2	3.9 ± 0.5	4.8 ± 0.65	82.3
Present work, MISC model[3]	52.3 ± 1.2	12.1 ± 0.52	8.8 ± 0.5	3.0 ± 0.4	3.8 ± 0.5	81

Notes: [1] MI model, constraints on the mass and the moment of inertia of the Moon

[2] MIS model, constraints on the mass, the moment of inertia, and the seismic velocities in the upper and the middle mantle. The values indicated in the upper lines are the constraints according to the model of Gagnepain-Beyneix et al. [2006], and those in the lower lines, according to the model in [Lognonné et al., 2005].

[3] MISC model, constraints on the mass, the moment of inertia, and the seismic velocities in the upper and the middle mantle plus the condition of similar concentrations in the upper and the middle mantle.

[1,2,3] –The values of concentrations and the corresponding errors in the present models are the mean values and the standard deviations calculated assuming normal distributions in the frequency histograms.

625–750 km quite well correlate with the modern models of the lunar constitution [Wieczorek et al., 2006; Khan et al., 2007]. To compare with, $H_{u-m} = 238$ km and $H_{m-l} = 738$ km in the work [Gagnepain-Beyneix et al., 2006]. According to the qualitative evaluation of the depth of the boundary between the middle and the lower mantle [Khan et al., 2007], $H_{m-l} = 500$–600 km for density and 800–900 km for S velocity; the boundary between the upper and the middle mantle is not recognized. Although the latter results testify in favor of the MISC model, one cannot definitely infer the absence of a weak chemical boundary at a depth of about 250 km from the work [Khan et al., 2007]. In our calculations on the MISC models, it is shown that the models of the Moon with a uniform chemical composition up to a depth of the lower mantle meet all the imposed constraints, just as the MIS models do. The mean seismic velocity profiles in the MIS and MISC models are almost identical (Table 1), which indicates that the identification of the chemical boundary between the upper and the middle mantle from the seismic constraints is a challenge. In our results, the question as to whether a weak chemical boundary exists at a depth of 250–300 km is left open.

6.7. The Silicate Portion of the Moon

Our results support the previous conclusions obtained by Kuskov and Kronrod [1998a; 1998b] about a qualitative difference between the bulk composition of the silicate Moon and the mantle of the Earth (Table 5). The whole range of the models considered relates to concentrations of FeO (9.9–12.1%) which are greater than those in the pyrolite (8.2%) [McDonough and Sun, 1995], although the mean concentrations of Al$_2$O$_3$ (3.8–4.8%) in the MIS and MISC models are close to pyrolite (4.5%) [McDonough and Sun, 1995]. The value of the magnesium number, which is one of the key geochemical parame-

ters, for the MIS models (MG#81−82) coincides with the estimates provided by the geochemical and geophysical models [Wänke and Dreibus, 1986; Taylor, 1982; Taylor at al., 2006; Khan et al., 2007; Kuskov, 1997; Kuskov and Kronrod, 1998a; 1998b]. This value is lower than the estimates commonly adopted for the Earth's mantle (MG#89.3) [McDonough and Sun, 1995], although higher than in the models [Lognonné et al., 2003] (MG#74.6). The major difference from the previous works [Kronrod and Kuskov, 1997; Kuskov and Kronrod, 1998a; 1998b; Kuskov et al., 2002] is smaller concentrations of Al_2O_3 in the bulk composition of the Moon, which is due to the particular formulations of the problem for the MIS and MISC models.

7. CONCLUSIONS

1. The constitution of the Moon, which was initially homogeneous and then experienced differentiation due to partial melting, is studied by numerical modeling. The mineral composition and physical properties of the lunar mantle are reconstructed by the Monte-Carlo inversion of the gravity and seismic constraints. The phase composition and the physical parameters of the mantle are calculated using the method of the Gibbs free energy minimization and the equations of state for the mantle material in the system $CaO-FeO-MgO-Al_2O_3-SiO_2$. The models of the Moon with a different degree of constraints on the desired solution are considered. In all models, the geophysically and geochemically permissible distributions of seismic velocities and chemical concentrations are determined for three mantle zones, and the radius of the Fe−10%S core is estimated. The effects in the solution, which are caused by the variations in the main input parameters of the models, are evaluated.

2. Based on the analysis of the models only constrained by the moment and the mass of the Moon, it has been shown qualitatively that the internal structure of the Moon is radially symmetric. Moreover, the seismic models and the zonal structure of the lunar interiors, which have been inferred from the local observations at the Apollo landing sites, apply for the entire Moon as well.

3. The main parameters of the lunar crust, the mantle, and the core are estimated. The crustal density is probably 2.9 g/cm^3, the crustal thickness is 50 km, and the radius of Fe−10%S core is 340 ± 30 km. The chemical boundary between the middle and the lower mantle is identified at a depth of 620−750 km. It is shown that the models of the Moon with and without a chemical boundary at a depth of 250−300 km are both possible. The seismic velocities at the depth of the lower mantle fall within the intervals $7.88 \le V_P \le 8.10$ km/s and $4.40 \le V_S \le 4.55$ km/s.

4. The mantle of the Moon is chemically stratified, and the concentrations of FeO, Al_2O_3 and CaO in the

different zones of the mantle, where orthopyroxene is the prevailing phase, are different. The silicate portion of the Moon (the crust and the mantle) probably contains 3.5−5.5% Al_2O_3 and 10.5−12.5% FeO.

REFERENCES

Arkani-Hamed, J., Viscosity of the Moon, *The Moon*, 1973, vol. 6, pp. 100−111.

Binder, A.B., The Initial Thermal State of the Moon, in *Origin of the Moon,* Hartmann, W.K. et al., Eds., Houston: Lunar Planet. Inst, 1986, pp. 425−433.

Delano, J.W., Pristine Lunar Glasses: Criteria Data, and Implications, *J. Geophys. Res.,* 1986, vol. 91, no. B4, pp. D201−D213.

Demidova, S.I., Nazarov, M.A., Lorents, K.A., et al., Chemical Composition of Lunar Meteorites and the Lunar Crust, *Petrologiya,* 2007, vol. 15, pp. 416−437 [*Petrology* (Engl. Transl.), 2007, vol. 15, no. 4, pp. 386−407].

Elkins, L.T., Fernandes, V.A., Delano, J.W., and Grove, T.L., Origin of Lunar Ultramafic Green Glasses: Constraints from Phase Equilibrium Studies, *Geochim. Cosmochim. Acta,* 2000, vol. 64, pp. 2339−2350.

Elkins-Tanton, L.T., Chatterjee, N., and Grove, T.L., Experimental and Petrologic Constraints on Lunar Differentiation from the Apollo 15 Green Picritic Glasses, *Meteorit. Planet. Sci,* 2003, vol. 38, pp. 515−527.

Gagnepain-Beyneix, J., Lognonné, P., Chenet, H., et al., A Seismic Model of the Lunar Mantle and Constraints on Temperature and Mineralogy, *Phys. Earth Planet. Inter.,* 2006, vol. 159, pp. 140−166.

Galimov, E.M., On the Origin of Lunar Material, *Geokhimiya,* 2004, no. 7, pp. 691−706 [*Geochem. Int.* (Engl. Transl.), 2004, vol. 42, no. 7, pp. 595−609].

Goins, N.R., Dainty, A.M., and Toksoz, M.N., Lunar Seismology: The Internal Structure of the Moon, *J. Geophys. Res.,* 1981, vol. 86, pp. 5061−5074.

Head, J.W. and Wilson, L., Lunar Mare Volcanism: Stratigraphy, Eruption Conditions, and Evolution of Secondary Crusts, *Geochim. Cosmochim. Acta,* 1992, vol. 56, pp. 2155−2176.

Hess, P.C. and Parmentier, E.M., A Model for the Thermal and Chemical Evolution of the Moon's Interior: Implications for the Onset of Mare Volcanism, *Earth Planet. Sci. Lett.,* 1995, vol. 134, pp. 501−514.

Hood, L.L. and Jones, J.H., Geophysical Constraints on Lunar Bulk Composition and Structure: A Reassessment, *J. Geophys. Res.,* 1987, vol. 92E, pp. 396 −410.

Hood, L.L. and Zuber, M., Recent Refinements in Geophysical Constraints on Lunar Origin and Evolution, in

Origin of the Earth and Moon, Righter K., Canup R., Eds., Tucson: Univ. Arizona Press, 2000, pp. 397–412.

James, O.B., Rocks of the Early Lunar Crust, *Proc. 11th Lunar Planet. Sci. Conf., Geochim. Cosmochim. Acta Suppl.* (Houston, 1980), New York: Pergammon Press, 1980, vol. 1, pp. 365–393.

Jones, J.H. and Delano, J.W., A Three-Component Model for the Bulk Composition of the Moon, *Geochim. Cosmochim. Acta,* 1989, vol. 53, pp. 513–527.

Khan, A., Mosegaard, K., and Rasmussen, K.L., A New Seismic Velocity Model for the Moon from a Monte Carlo Inversion of the Apollo Lunar Seismic Data, *Geophys. Rev. Lett.,* 2000, vol. 27, pp. 1591–1594.

Khan, A. and Mosegaard, K., An Inquiry Into the Lunar Interior: a Nonlinear Inversion of the Apollo Lunar Seismic Data, *J. Geophys. Res,* 2002, vol. 107, no. E6, pp. 5036–5059.

Khan, A., Connolly, J.A.D., Olsen, N., and Mosegaard, K., Constraining the Composition and Thermal State of the Moon from An Inversion of Electromagnetic Lunar Day-Side Transfer Functions, *Earth Planet. Sci. Lett.,* 2006a, vol. 248, pp. 579–598.

Khan, A., Maclennan, J., Taylor, S. R., and Connolly, J. A. D. Are the Earth and the Moon Compositionally Alike? Inferences on Lunar Composition and Implications for Lunar Origin and Evolution from Geophysical Modeling, *J. Geophys. Res.,* 2006b, vol. 111, p. E05005, doi:10.1029/ 2005JE002608.

Khan, A., Connolly, J.A.D., Maclennan, J., and Mosegaard, K., Joint Inversion of Seismic and Gravity Data for Lunar Composition and Thermal State, *Geophys. J. Int.,* 2007, vol. 168, pp. 243–258.

Kirk, R.L. and Stevenson, D.J., The Competition Between Thermal Contraction and Differentiation in the Stress History of the Moon, *J. Geophys. Res.,* 1989, vol. 94, pp. 12 133–12 144.

Konopliv, A.S., Binder, A.B., Hood, L.L., et al., Improved Gravity Field of the Moon from Lunar Prospector, *Science,* 1998, vol. 281, pp. 1476–1480.

Kronrod, V.A. and Kuskov, O.L., Chemical Composition, Temperature, and Radius of the Lunar Core from Geophysical Evidence, *Geokhimiya,* 1997, no. 2, pp. 4–12 [*Geochem. Int.* (Engl. Transl.), 1997, vol. 35, no. 2, pp. 104–112].

Kronrod, V.A. and Kuskov, O.L., Temperature in the Moon's Mantle from Seismic Data, *Fiz. Zemli,* 1999, no. 5, pp. 363–371 [*Izv. Phys. Earth* (Engl. Transl.), 1999, vol. 35, no. 5, pp. 363–371].

Kronrod, V.A. and Kuskov, O., L., Modeling of the Thermal Structure of Continental Lithosphere, *Fiz. Zemli,* 2007, no. 1, pp. 96–107 [*Izv. Phys. Earth* (Engl. Transl.), 2007, vol. 43, no. 1, pp. 91–101].

Kuskov, O.L., Constitution of the Moon: 4. Composition of the Mantle from Seismic Data, *Phys. Earth Planet. Inter.,* 1997, vol. 102, pp. 239–257.

Kuskov, O.L. and Kronrod, V.A., Constitution of the Moon: 5. Constraints on Composition, Density, Temperature, and Radius of a Core, *Phys. Earth Planet. Inter.,* 1998a, vol. 107, pp. 285–306.

Kuskov, O.L. and Kronrod, V.A., A Model of the Chemical Differentiation of the Moon, *Petrologiya,* 1998b, vol. 6,

pp. 616–633 [*Petrology* (Engl. Transl.), 1998b, vol. 6, no. 6, pp. 564–582].

Kuskov, O.L. and Kronrod, V.A., The Moon: Chemical Composition and Internal Structure, *Solar Syst. Res.,* 1999, vol. 33, pp. 382–391.

Kuskov, O.L. and Kronrod, V.A., Resemblance and Difference Between Constitution of the Moon and Io, *Planet. Space Sci.,* 2000, vol. 48, pp. 717–726.

Kuskov, O.L. and Kronrod, V.A., Core Sizes and Internal Structure of the Earth's and Jupiter's Satellites, *Icarus,* 2001, vol. 151, pp. 204–227.

Kuskov, O.L., Kronrod, V.A., and Hood, L.L., Geochemical Constraints on the Seismic Properties of the Lunar Mantle, *Phys. Earth Planet. Inter.,* 2002, vol. 134, pp. 175–189.

Kuskov, O.L., Kronrod, V.A., and Annersten, H., Inferring Upper-Mantle Temperatures from Seismic and Geochemical Constraints: Implications for Kaapvaal Craton, *Earth Planet. Sci. Lett.,* 2006, vol. 244, pp. 133–154.

Kuskov, O.L., Dorofeeva, V.A., Kronrod, V.A., and Makalkin, A.B., *Sistemy Yupitera i Saturna: formirovanie, sostav i vnutrennee stroenie krupnykh sputnikov* (Jupiter and Saturn Systems: Formation, Composition, and Internal Structure of Large Satellites), Moscow: Izd-vo LKI, 2009.

Kuskov, O.L. and Kronrod, V.A., Geochemical Constraints on the Model of the Composition and Thermal Conditions of the Moon according to Seismic Data, *Fiz. Zemli,* 2009, no. 9, pp. 25–40 [*Izv. Phys. Earth* (Engl. Transl.), 2009, vol. 45, no. 9, pp. 753–768].

Latham, G., Ewing, M., Dorman, J., et al., Moonquakes and Lunar Tectonism, *The Moon,* 1972, vol. 4, pp. 373–382.

Lognonné, P., Gagnepain-Beyneix, J., and Chenet, H., A New Seismic Model of the Moon: Implications for Structure, Thermal Evolution and Formation of the Moon, *Earth Planet. Sci. Lett.,* 2003, vol. 211, pp. 27–44.

Lognonné, P., Planetary Seismology, *Annu. Rev. Earth Planet. Sci,* 2005, vol. 33, pp. 571–604.

Longhi, J., Experimental Petrology and Petrogenesis of Mare Volcanics, *Geochim. Cosmochim. Acta,* 1992, vol. 56, pp. 2235–2251.

McDonough, W.F. and Sun, S.-s., The Composition of the Earth, *Chem. Geol.,* 1995, vol. 120, pp. 223–253.

Nakamura, Y. and Koyama, J., Seismic Q of the Lunar Upper Mantle, *J. Geophys. Res.,* 1982, vol. 87, pp. 4855–4861.

Nakamura, Y., Seismic Velocity Structure of the Lunar Mantle, *J. Geophys. Res.,* 1983, vol. 88, pp. 677–686.

O'Neill, H.St.C., The Origin of the Moon and the Early History of the Earth—A Chemical Model. Part 1: The Moon, *Geochim. Cosmochim. Acta,* 1991, vol. 55, pp. 1135–1157.

Ringwood, A.E. and Essene, E., Petrogenesis of Apollo 11 Basalts, Internal Constitution and Origin of the Moon, *Proc. Apollo 11th Lunar Planet. Sci. Conf., Geochim. Cosmochim. Acta Suppl.* (Houston, 1970), Levinson, A.A., Ed., New York: Pergammon Press, 1970, vol. 1, pp. 769–799.

Ringwood, A.E., *Origin of the Earth and Moon,* New York: Springer, 1979.

Sambridge, M. and Mosegaard, K., Monte Carlo Methods in Geophysical Inverse Problems, *Rev. Geophys.,* 2002, vol. 40, no. 3, pp. 1–29.

Shearer, C.K. and Papike, J.J., Basaltic Magmatism on the Moon: A Perspective from Picritic Glass Beads, *Geochim. Cosmochim. Acta,* 1993, vol. 57, pp. 4785–4812.

Shearer, C.K. and Papike, J.J., Magmatic Evolution of the Moon, *Am. Mineral.,* 1999, vol. 84, pp. 1469–1494.

Solomon, S.C., On the Early Thermal State of the Moon, in *Origin of the Moon,* Hartmann, W.K. et al., Eds., Houston: LPI, 1986, pp. 435–452.

Taylor, S.R., *Planetary Science: A Lunar Perspective,* Houston: LPI, 1982.

Taylor, S.R., The Origin of the Moon: Geochemical Considerations, in *Origin of the Moon,* Hartmann, W.K. et al., Eds., Houston: LPI, 1986, pp. 125–143.

Taylor, S.R., Taylor, G.J., and Taylor, L.A., The Moon: A Taylor Perspective, *Geochim. Cosmochim. Acta,* 2006, vol. 70, pp. 5904–5918.

Vanyan, L.L. and Egorov, I.V., The Lunar Lithosphere from Electromagnetic Sounding Data, *The Moon,* 1977, vol. 17, pp. 3–9.

Wänke, H. and Dreibus G., Geochemical Evidence for the Formation of the Moon by Impact-Induced Fission of the Proto-Earth, in *Origin of the Moon,* Hartmann, W.K. et al., Eds., Houston: LPI, 1986, p. 649–672.

Wieczorek, M.A. and Phillips, R.J., The "Procellarum KREEP Terrane": Implications for Mare Volcanism and Lunar Evolution, *J. Geophys. Res.,* 2000, vol. 105, no. E8, pp. 20 417–20 430.

Wieczorek, M.A., Jolliff, B.L., Khan, A., et al., The Constitution and Structure of the Lunar Interior, *Rev. Mineral. Geochem.,* 2006, vol. 60, no. 1, pp. 221–364.